AIAA/AAS Astrodynamics Specialist Conference and Exhibit
5-8 August 2002, Monterey, California

AIAA 2002-4890

Time Series Analysis of HASDM Thermospheric Temperature and Density Corrections

Bruce R. Bowman
Mark F. Storz

Air Force Space Command, Space Analysis Center
Peterson AFB, Colorado 80914-4650

Abstract

The Dynamic Calibration Atmosphere (DCA) is the algorithm that estimates the temperature/density correction coefficients for the High Accuracy Satellite Drag Model initiative. Here we analyze both the time series of these coefficients and the effect applying them has on the estimated ballistic coefficients. The spatial coverage and temporal data density for the calibration satellites was adequate for obtaining reliable estimates for the model corrections. For this study, the primary metric for evaluating the success of the coefficients in correcting the model density is the difference between the *a priori* 'true' ballistic coefficient and the estimated ballistic coefficient after the DCA density correction is applied. The smaller this ballistic coefficient difference, the better the density correction. The results indicate that the coefficients successfully correct the density at all satellite altitudes and inclinations. In particular, it is shown that at least two temperature parameters are needed to produce a density correction profile that adequately fits the satellite drag data. Once these parameters were chosen, each was estimated in terms of a separate and independent spherical harmonic expansion with latitude and local solar time. The time series of the resulting spherical harmonic coefficients were also analyzed qualitatively to describe their variability in response to changes in extreme ultra-violet (EUV) heating and geomagnetic Joule heating. The responses are consistent enough that the basic density model can be significantly improved, either by adjusting the empirical equations within the model or by adding a coefficient prediction filter to the model.

Introduction

The High Accuracy Satellite Drag Model (HASDM) (Storz, 2002) uses a modified Jacchia 70 model atmosphere (Jacchia, 1970) for density and satellite drag computations. Spherical harmonic expansions in the nighttime minimum exospheric temperature T_c (> 600 km altitude) and the inflection point temperature T_x (at 125 km altitude) are used to represent corrections in the temperature field. These expansions are formulated as a function of latitude and local solar time. The temperature corrections lead to density corrections through integration of the hydrostatic and diffusion equations. These corrections are estimated in the HASDM orbit/density correction process using drag information from 75 calibration satellites. This process is known as the Dynamic Calibration Atmosphere (DCA) (Casali, 2002). Table 1 shows the range of orbit inclinations and perigee heights selected for the calibration group. These 75 satellites were observed multiple times almost every revolution by the Space Surveillance Network of radar and optical trackers. An average of 500 observations per day per satellite were fitted in the DCA least squares orbit/density determination process to estimate the spherical harmonic temperature/density corrections.

Height Min:	190	250	300	400	500	600	700
(km) Max:	250	300	400	500	600	700	900
Inclination:							
20-30	2	3	2				
30-40	5			2			
40-50	1		3	1	2	1	
50-60	1	1	1		1		
60-70				3			3
70-80		1	4	1			
80-100		2	6	6	13	6	4
Total	9	7	16	13	16	7	7

Table 1. HASDM calibration satellites' orbit parameters.

This paper reveals the changes in the estimated ballistic coefficients due to the unmodeled atmospheric density variations, and describes the computed temperature corrections required to account for the unmodeled effects. This paper includes an evaluation of the effect the density correction has on the time histories of the estimated ballistic coefficients after the corrections are applied to the orbit determination process.

Ballistic Coefficient and Atmospheric Density Analysis

The Jacchia 70 model is known (Marcos, 1990) to have large density errors with standard deviations of about 15% for orbits at approximately 400 km altitude. The unmodeled errors in density are aliased into estimated ballistic coefficient B′ variations because of the direct proportionality of B′ with density when computing drag accelerations. The prime (′) is used to distinguish the estimated ballistic coefficient from the 'true' ballistic coefficient B. Therefore, the change in B′ directly reflects the unmodeled density correction that is required, assuming that the satellite does not have long-term variations in frontal area. Figure 1 shows the changes in the estimated ballistic coefficient averaged over sets of satellites grouped according to altitude range. The ΔB/B value is the percent change in B′ with respect to the 'true' long-term B value of the satellite, where ΔB = B′- B. The 'true' B is obtained as an approximation from a 31-year average of the estimated B′ values (Bowman, 2002). Each ΔB/B curve in Figure 1 represents an average of three or four different satellite's having different inclinations, but approximately the same perigee altitude. The ΔB/B curves range from 160 km to 560 km in altitude. Each curve has been shifted by 20% from the altitude curve just below it. The shift was done for clarity to show how the variations in B′ change with altitude. The ΔB/B (*i.e.* density) changes shown in Figure 1 reveal the unmodeled variations of the Jacchia 70 density as a function of altitude. For low altitudes the unmodeled variations in the density mainly result from geomagnetic storm responses, while at higher altitudes, the unmodeled variations are mainly a result of incorrectly modeled $F_{10.7}$ responses. At the very low altitudes, the unmodeled $F_{10.7}$ variations, that are readily visible at higher altitudes, have almost disappeared. Figure 2 shows the B′ variations at altitudes from 210 km to 560 km for a group of low inclination satellites. High inclination satellites were not selected for this comparison because of the large density changes that can occur at high latitudes during geomagnetic storms due to auroral oval Joule heating. The legend lists the satellite numbers, the orbit inclination (inclination in parentheses is for a retrograde orbit), and the perigee height. The B′ variations from day 25 to 65 are anomalous. The $F_{10.7}$ variation during this time is almost non-existent, and the ΔB/B values (*i.e.* density errors) have a very distinct separation with altitude. During this time period the Jacchia 70 model underestimates the density increasingly as a function of altitude. As soon as the $F_{10.7}$ variation increases after day 65, density variations at different altitudes converge and vary in unison. However, there is an anti-correlation of the ΔB/B change with respect to the $F_{10.7}$ variation. This indicates that at the $F_{10.7}$ maximum values, Jacchia overestimated the density, and at the $F_{10.7}$ minima, Jacchia underestimated the density. It is interesting to note that, in general, a density separation with height occurs even during the times of large $F_{10.7}$ variation. The main point is that the HASDM temperature corrections need to account for a wide variety of density variations throughout the drag altitude regime.

Temperature Validation

The best HASDM-derived temperature field (2×2 in ΔT_c and 1×1 in ΔT_x) was used to recompute B′ values for a number of satellites. The derived temperature data was used as input along with the original solar indices into the modified Jacchia 70 correction model to compute new B′ values throughout the HASDM time period. If the global temperature corrections account for all the mis-modeling in the Jacchia 70 model then the ΔB/B variations should be near zero.

The lowest perigee altitude satellites were examined first. The very low altitude satellites are especially subject to mis-modeling during geomagnetic storms, as seen in Figure 1. Figure 3 shows the original B′ values (without the temperature correction coefficients applied) for the lowest altitude group of calibration satellites. The ΔB/B values of the four satellites, with perigee altitudes from 195 km to 210 km, show that temperature/density corrections to the Jacchia model are required during periods of strong geomagnetic activity. Four large geomagnetic storms occurred during March and April of 2001 (from day 80 to 108). The B′ term response from different satellites varies, depending upon perigee location. Satellites with perigee locations within 15° of the auroral oval exhibit larger B′ variations during geomagnetic storms. The largest variations in B′ are for satellite 19348, which has a perigee location at the most southern part of the orbit, –47° latitude, during the storm times. Satellite 06073 has a perigee location at the most northern part of its orbit, +52° latitude, during the same time period. All four satellites have apogees of at least 5000 km, which means that the great majority of their drag occurs at the perigee location. The most outstanding difference in the B′ variations is the difference in the storm responses. Even though the day 90 event is by

far the largest storm, the Jacchia model seems to have modeled this better than the other 3 major storms. The day 80 event, the smallest of the four storms, has the largest response in the B′ change from satellite 19348. The data indicates additional density variations occurring that are not modeled directly as a function of the a_p index. The anti-correlation of B′ change with respect to the $F_{10.7}$ index observed in Figure 2 is almost damped out at these altitudes. It is still present, but with a very small amplitude.

Figure 4 shows the new B′ values once the global temperature/density correction field has been applied. It was determined that the ΔT_x contribution to the global correction field produces a greater effect the lower the perigee altitude. The best solution for ΔT_x was a 1×1 field. In using the best correction field, all the new B′ values have been reduced significantly from the original values in Figure 3. Even during the storm times the B′ fluctuations have been greatly reduced relative to the true ballistic coefficient B. This implies that the global temperature/density correction field is successfully correcting the model density.

Figure 5 shows the uncorrected B′ variations for another group of calibration satellites in the 210 km to 240 km perigee altitude range. Again, one can see that the Jacchia 70 model needs to be corrected to account for the a_p variations, and also to account for the additional unmodeled $F_{10.7}$ variations that are starting to appear as the perigee altitude is increased. The anti-correlation of B′ change with respect to $F_{10.7}$ is more easily observable than in the previous satellite group. It is surprising that, with an increase of only 20 to 40 km in perigee altitude, this $F_{10.7}$ anti-correlation becomes so readily observable. Figure 6 shows the new B′ values once the global temperature field has been applied. As with the group of lower perigee altitude satellites, the global temperature field has done an excellent job of correcting the Jacchia unmodeled variations so that B′ is very close to the 'true' B.

Finally, a number of low inclination satellites were selected for evaluation of the global temperature field. The perigee altitudes for this group ranged from 260 km to 560 km. None of this group included any calibration satellites that were used to solve for the temperature coefficients. Figure 2 shows the uncorrected variations in B′ for this group. The B′ variations are as much as 65% for the high altitude Vanguard 2 sphere, satellite 00011. Figure 7 shows the B′ values determined from the temperature/density correction field. The standard deviations are all less than 7% for all altitudes. This indicates that the correction field can be readily applied to satellites from low to high perigee altitudes with consistent favorable results.

Temperature Coefficients

The temperature field determined to best fit the calibration satellite data was 2×2 (9 coefficients) for the nighttime minimum exospheric temperature correction ΔT_c together with 1×1 (4 coefficients) for the inflection point temperature correction ΔT_x. The spherical harmonic expansion for ΔT_c may be expressed as:

$$\Delta T_c(\phi,\lambda) = \hat{C}_{00} + \sum_{n=1}^{N}\left[\sum_{m=0}^{n}\hat{C}_{nm}P_{nm}(z)\cos(m\lambda) + \sum_{m=1}^{n}\hat{S}_{nm}P_{nm}(z)\sin(m\lambda)\right]$$

where ϕ is the geocentric latitude, λ is the local solar time expressed as an angle, and $z = \sin\phi$.

The spherical harmonic expansion for ΔT_x may be similarly expressed as:

$$\Delta T_x(\phi,\lambda) = \tilde{C}_{00} + \sum_{n=1}^{N}\left[\sum_{m=0}^{n}\tilde{C}_{nm}P_{nm}(z)\cos(m\lambda) + \sum_{m=1}^{n}\tilde{S}_{nm}P_{nm}(z)\sin(m\lambda)\right]$$

$\hat{C}_{nm}$ and $\tilde{C}_{nm}$ are coefficients for the even spherical harmonic functions dependent on $\cos(m\lambda)$. $\hat{S}_{nm}$ and $\tilde{S}_{nm}$ are coefficients for the odd spherical harmonic functions dependent on $\sin(m\lambda)$.

The hat symbol $\wedge$ identifies coefficients for the correction to nighttime minimum exospheric temperature ΔT_c and the tilde symbol ~ identifies coefficients for the correction to inflection point temperature ΔT_x. Here, n is the degree and m is the order of the spherical harmonic term. The functions P_{n0} are the normalized Legendre functions (polynomials) and the functions P_{nm}, $m > 0$, are the normalized associated Legendre functions [5]. There are a total of $(N+1)^2$ terms in a particular spherical harmonic series truncated to degree N.

Figure 8 shows a plot of the degree 0 term ($\hat{C}_{00}$) for ΔT_c, including its 10-day average. The anti-correlation of $\hat{C}_{00}$ with the $F_{10.7}$ index is readily apparent. This term corrects the large anti-correlation of density with respect to $F_{10.7}$ seen in the previously described figures. The term also appears

to account for the mis-modeling of the different geomagnetic events. Figure 9 is a blowup of the $\hat{C}_{00}$ plot for the geomagnetic events time period. Figure 10 is the degree 0 term ($\tilde{C}_{00}$) for ΔT_x plot for the same time period. From Figures 9 and 10 it is obvious that the geomagnetic storms do not produce the same density variations. Both the ΔT_c and ΔT_x degree 0 temperature corrections show an increase for the day 80 storm, while there does not appear to be any significant ΔT_c increase for the large day 90 storm. For the day 102 event there is a very large increase in the ΔT_x inflection point temperature. All this points to the fact that a_p does not represent all the heating that is occurring during these geomagnetic events.

The following is a description of the time series for each of the zero degree spherical harmonic coefficients, one for the nighttime minimum exospheric temperature correction ΔT_c and one for the inflection point temperature correction ΔT_x, respectively.

- $\hat{C}_{00}$ exhibits a strong positive correlation with a_p. This indicates that the standard Jacchia 1970 model underestimates the thermospheric density during geomagnetic storms. However, this coefficient exhibits a significant anti-correlation with respect to enhancements in $F_{10.7}$.
- $\tilde{C}_{00}$ appears to have a negative reaction to the initial phase of the geomagnetic storm, followed by a positive reaction. There also appears to be a positive correlation of this coefficient with the semiannual variation showing a peak in the spring and another in the autumn.

The current analysis focused on the low perigee altitude satellites, which were more difficult to fit with the temperature field than for satellites with perigees higher than 300 km. The best temperature field fit for the low altitude satellites consisted of using a first degree term in ΔT_x along with the zero degree term. The following is a description of the time series for each of the first degree spherical harmonic coefficients for the inflection point temperature correction ΔT_x:

- $\tilde{C}_{10}$ exhibits a weak positive correlation with enhanced a_p during geomagnetic storms. A curious period of significantly negative values occurs between days 150 and 170. This is the period when $\hat{C}_{10}$ exhibits unusually positive values, thus exhibiting anti-correlation between ΔT_c and ΔT_x for this coefficient.
- $\tilde{C}_{11}$ exhibits a strong positive correlation with geomagnetic storms depending upon which storm is analyzed.
- $\tilde{S}_{11}$ also exhibits a strong positive reaction to geomagnetic storms, again depending upon which storm is analyzed. In contrast to $\tilde{C}_{10}$, this coefficient exhibits a period of significantly positive values between days 150 and 170. This is the period when $\hat{S}_{11}$ exhibits unusually positive values, thus exhibiting anti-correlation between ΔT_c and ΔT_x for this coefficient also.

The description of the time series for the other spherical harmonic coefficients not covered in this paper can be found in the HASDM validation tool paper (Storz, M., 2002).

Conclusion

Temperature/density correction coefficients from the Dynamic Calibration Atmosphere (DCA) were evaluated. We analyzed both the time series of these coefficients, and the effect applying these coefficients has on the time series of estimated ballistic coefficients. The spatial coverage and temporal data density for the calibration satellites is sufficient for estimating reliable spherical harmonic temperature/density coefficients up to degree 2 for the nighttime minimum exospheric temperature correction ΔT_c , and up to degree 1 for the inflection point temperature correction ΔT_x . The primary metric for evaluating the success of the coefficients in correcting the model density is the difference between the *a priori* 'true' ballistic coefficient and the estimated ballistic coefficient after the density correction is applied. The smaller this ballistic coefficient difference, the better the density correction. The standard deviation associated with the time series of ΔB/B was typically reduced about 4-fold, with the exception of very low altitudes (perigees < 250 km), where the reduction of the standard deviation is about 3-fold. The results indicate that the coefficients successfully correct the density at all satellite altitudes and inclinations. In particular, it was shown that at least two temperature parameters are needed to produce a density correction profile that adequately fits the satellite drag data. The time series of the coefficients themselves were also analyzed qualitatively to describe their variability in response to changes in extreme ultraviolet (EUV) heating and geomagnetic Joule heating. The response is consistent enough for the basic density model to be significantly improved; either through reformulation of the empirical equations of the baseline thermospheric density model (Jacchia 70), or by adding a prediction filter describing how the coefficients change with the input energy indices, as well as the time histories of the coefficients themselves.

Acknowledgment

We would like to thank Mr. William Barker and Mr. Stephen Casali of Omitron Inc., Dr. Kent Tobiska of Space Environment Research, Inc., and Mr. Frank Marcos of Air Force Research Laboratory for their valuable contributions and insight.

References

Bowman, B. R., "True Satellite Ballistic Coefficient Determination for HASDM,"AIAA-2002-4887, *AIAA/AAS Astrodynamics Specialist Conference*, Monterey,California, August, 2002.

Casali,S. , W. Barker, "Dynamic Calibration Atmosphere (DCA) for the High Accuracy Satellite Drag Model (HASDM)," AIAA-2002-4888, *AIAA/AAS Astrodynamics Specialist Conference*, Monterey, California, August, 2002.

Jacchia, L. G., New Static Models of the Thermosphere and Exosphere with Empirical Temperature Profiles, *Smithson. Astrophys. Special Report 313*, 1970.

Marcos, F. A., "Accuracy of Atmospheric Drag Models at Low Satellite Altitudes," *Adv. Space Research*, **10**, (3) pp. 417-422, 1990.

Storz, M., B. R. Bowman, and J. I. Branson, "High Accuracy Satellite Drag Model (HASDM)," AIAA-2002-4886, *AIAA/AAS Astrodynamics Specialist Conference*, Monterey, California, August, 2002.

Storz, M., "HASDM Validation Tool Using Energy Dissipation Rates," AIAA-2002-4889, *AIAA/AAS Astrodynamics Specialist Conference*, Monterey, California, August, 2002.

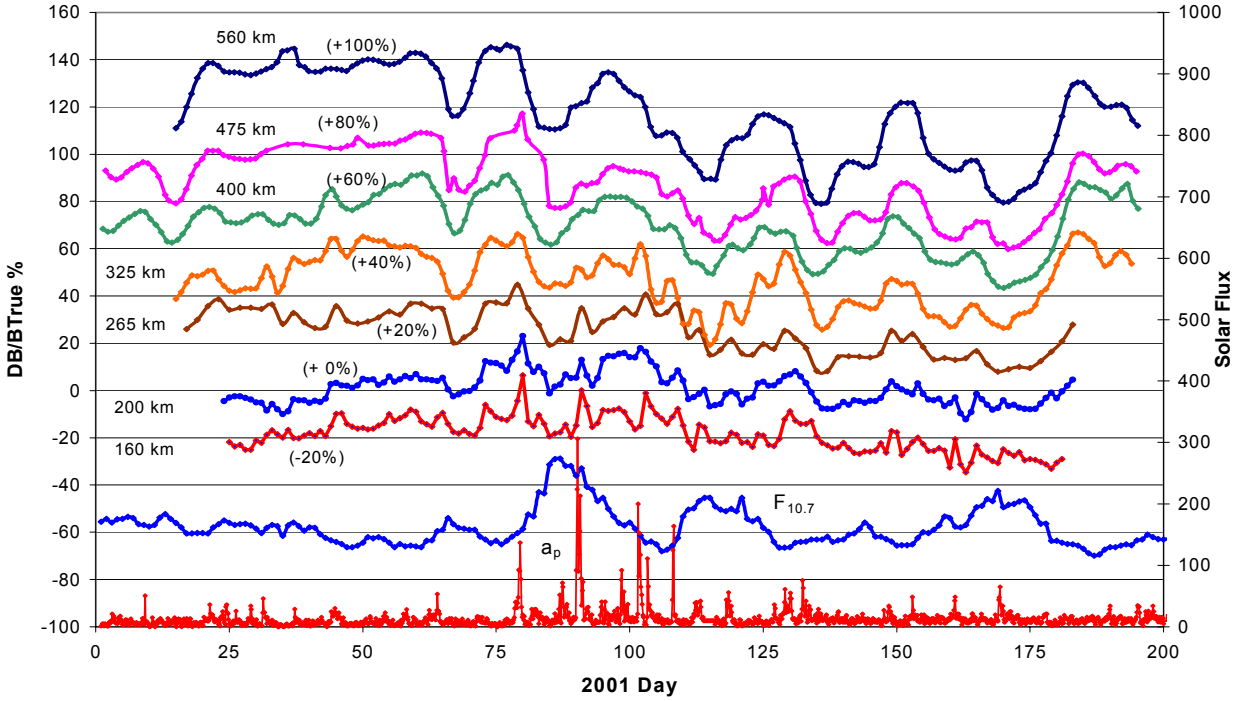

Figure 1. 2001 Average $\Delta B / BTrue$ values for satellite altitude groups. Each curve is shifted by +20% from the lower curve for clarity.

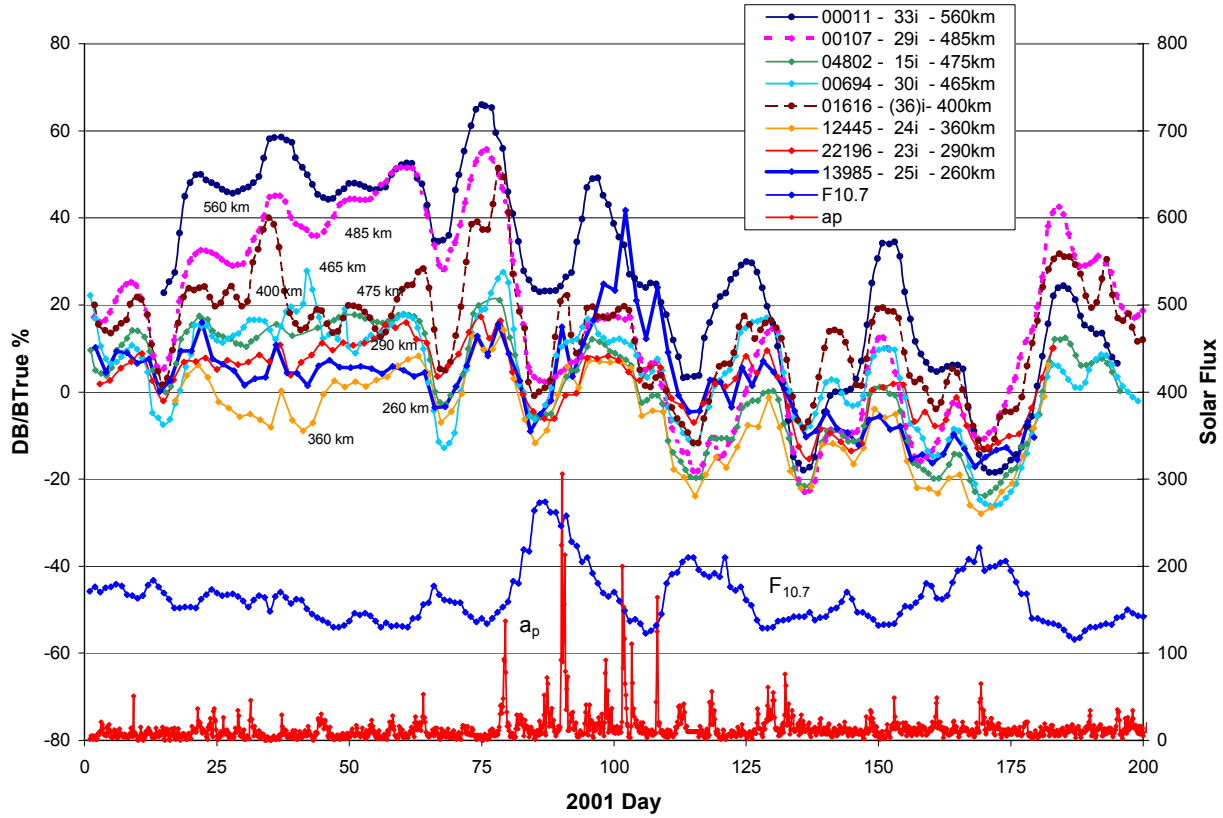

Figure 2. 2001 $\Delta B / BTrue$ values for a group of low inclination evaluation satellites at perigee heights from 260 km to 560 km.

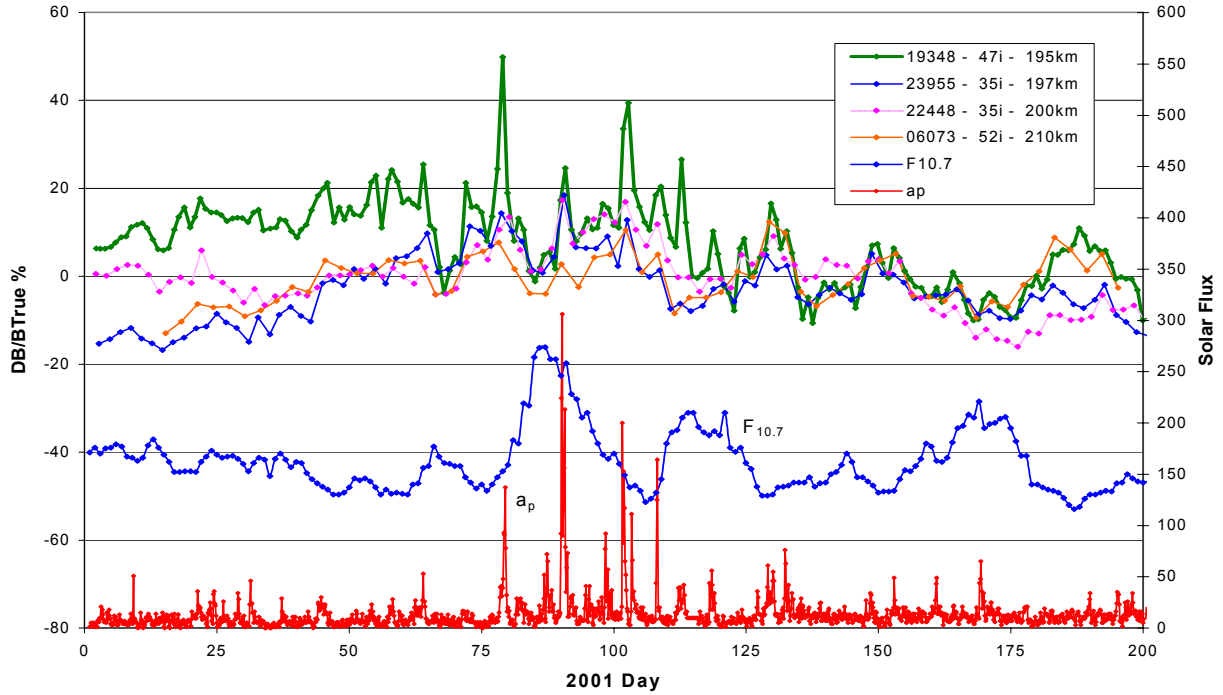

Figure 3. 2001 ΔB / *BTrue* values for low perigee height (195 km to 210 km) HASDM calibration satellites.

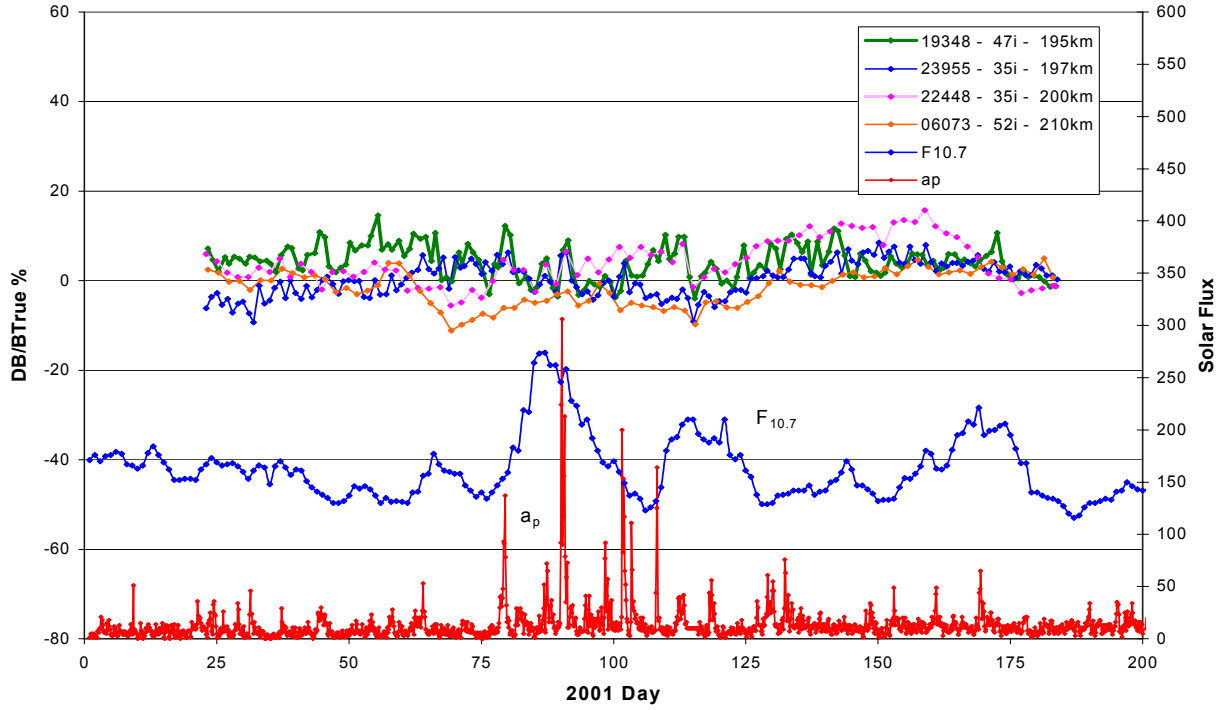

Figure 4. 2001 ΔB / *BTrue* values after the DCA 2x1 temperature corrections were applied for low perigee height (195 km to 210 km) HASDM calibration satellites.

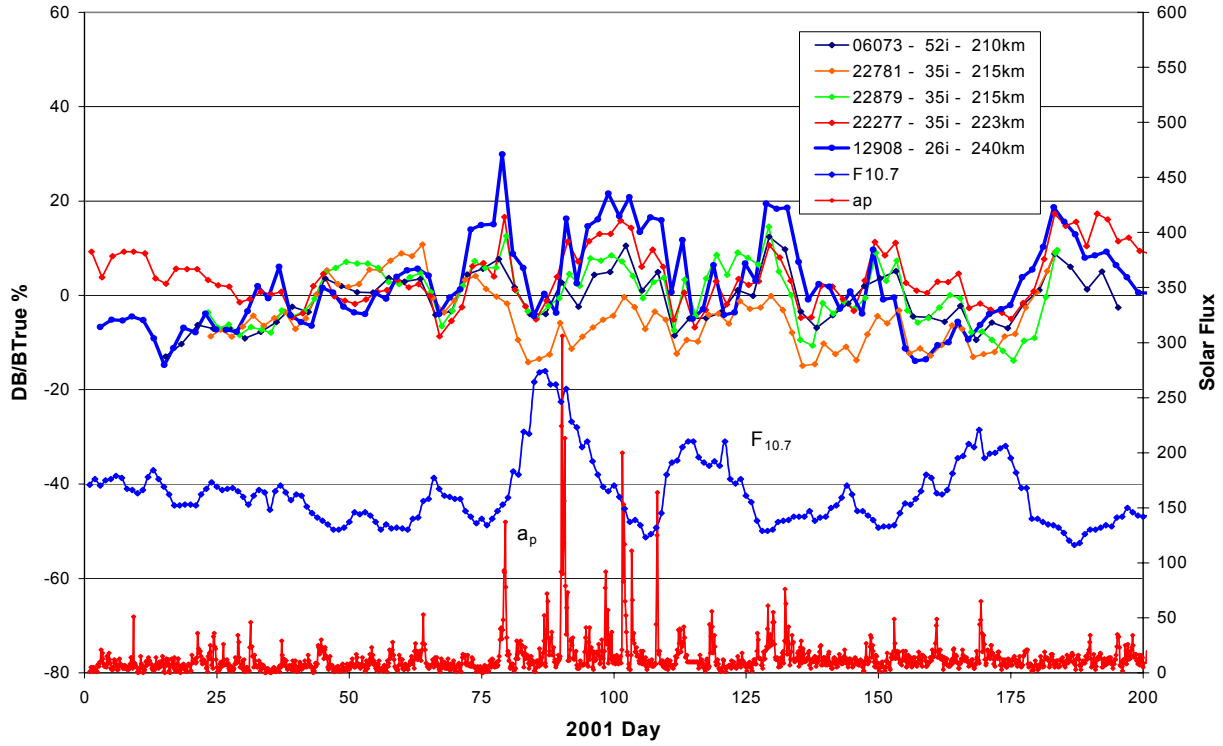

Figure 5. 2001 ΔB / *BTrue* values for low perigee height (210 km to 240 km) HASDM calibration satellites.

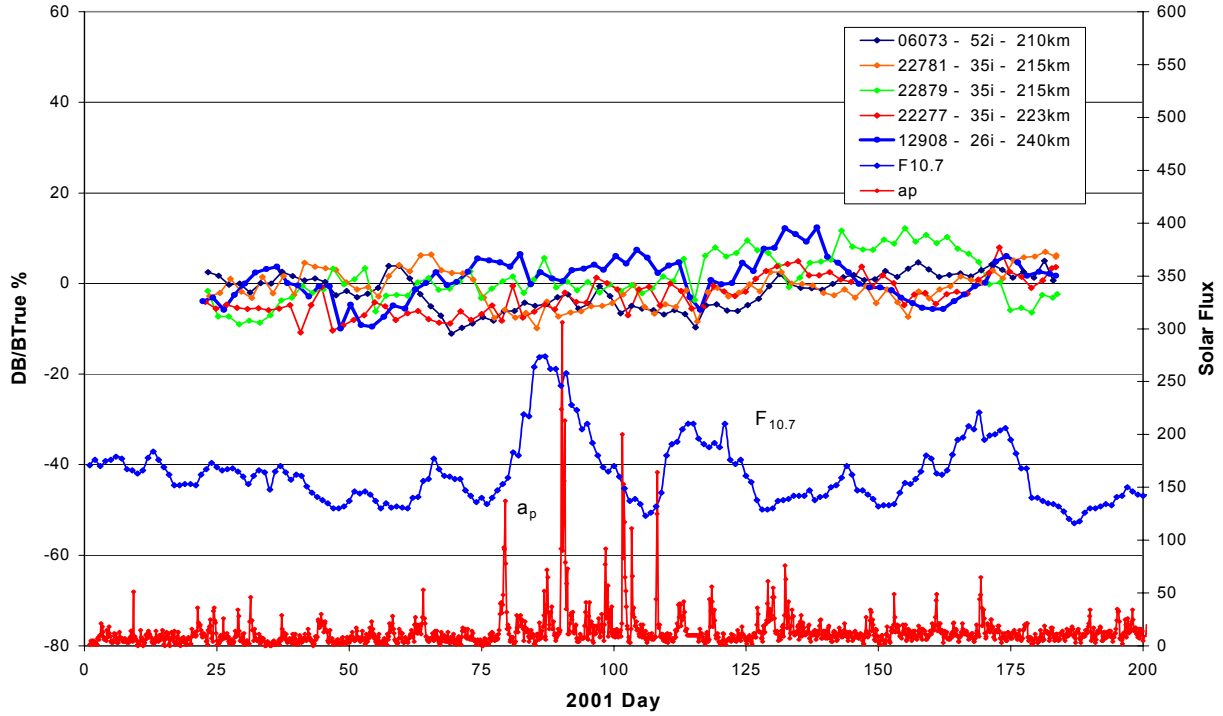

Figure 6. 2001 ΔB / *BTrue* values after the DCA 2x1 temperature corrections were applied for low perigee height (210 km to 240 km) HASDM calibration satellites.

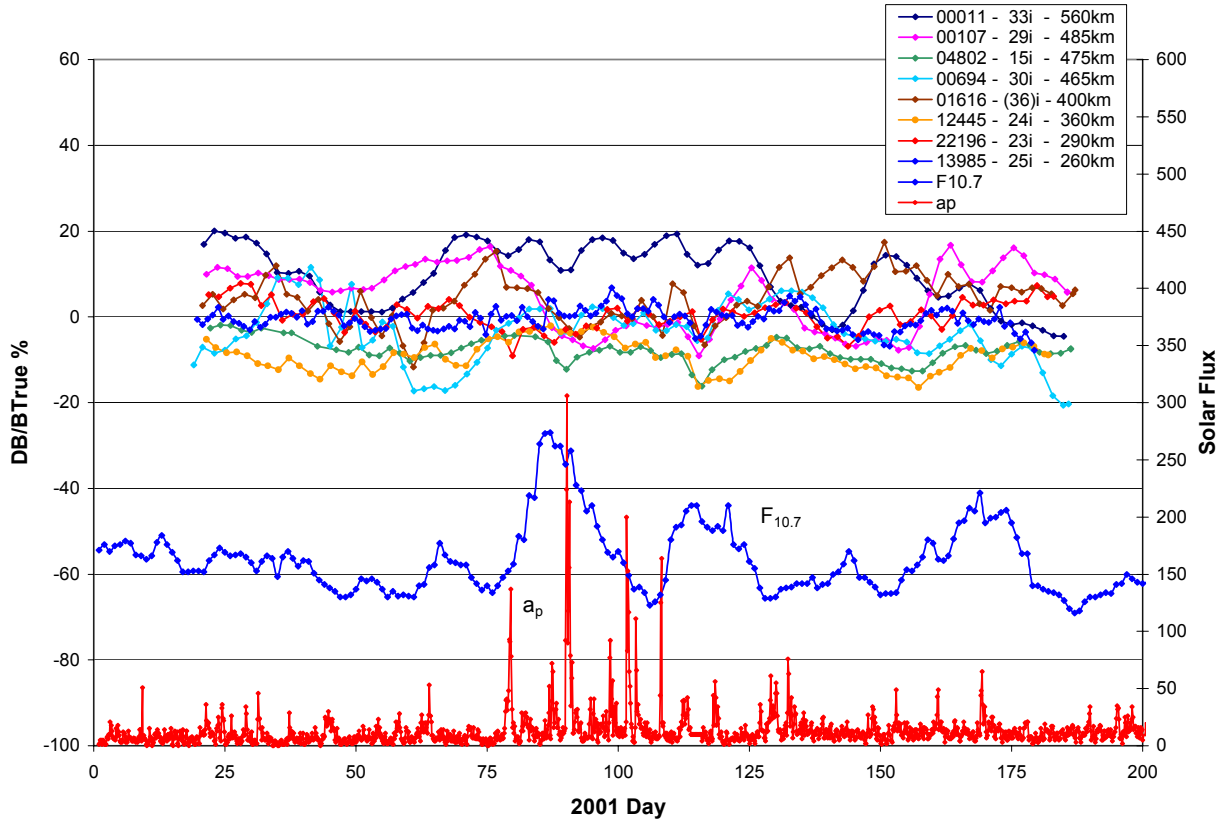

Figure 7. 2001 $\Delta B / BTrue$ values after the DCA 2x1 temperature corrections were applied for a group of low inclination evaluation satellites with perigee heights from 260 km to 560 km.

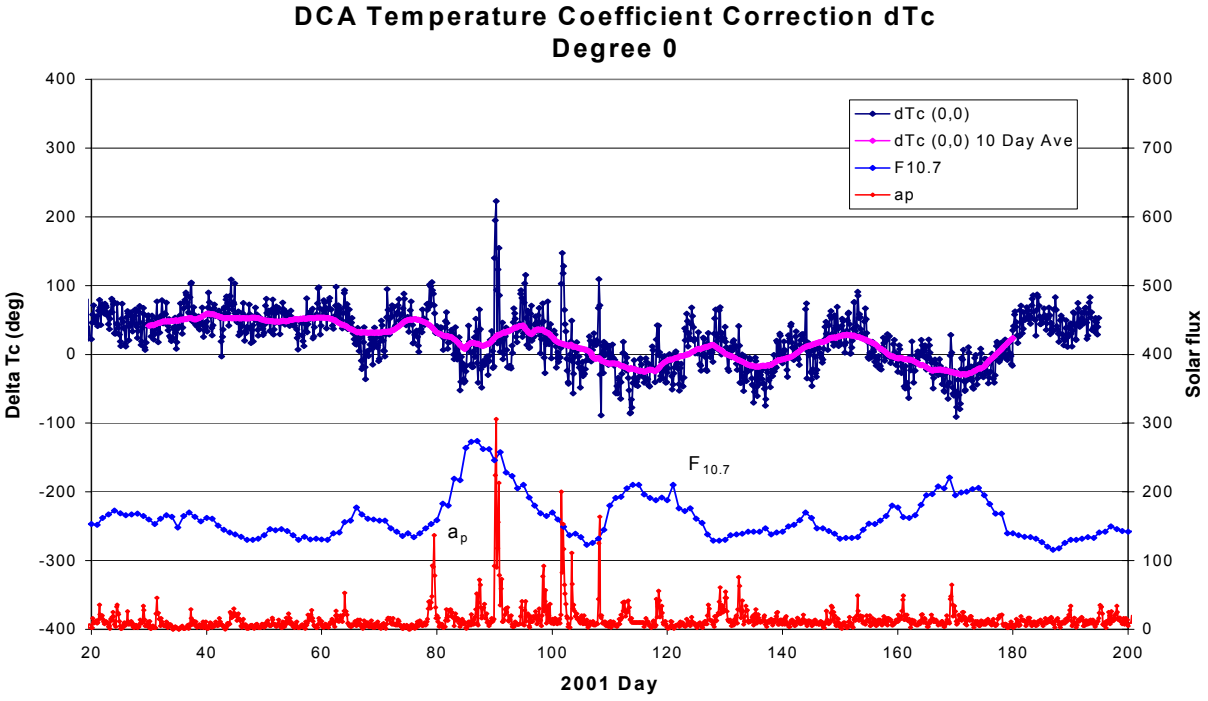

Figure 8. 2001 days 20 to 200 ΔT_c values from the degree 0 DCA 2x1 temperature field. The 10 day average values are also included.

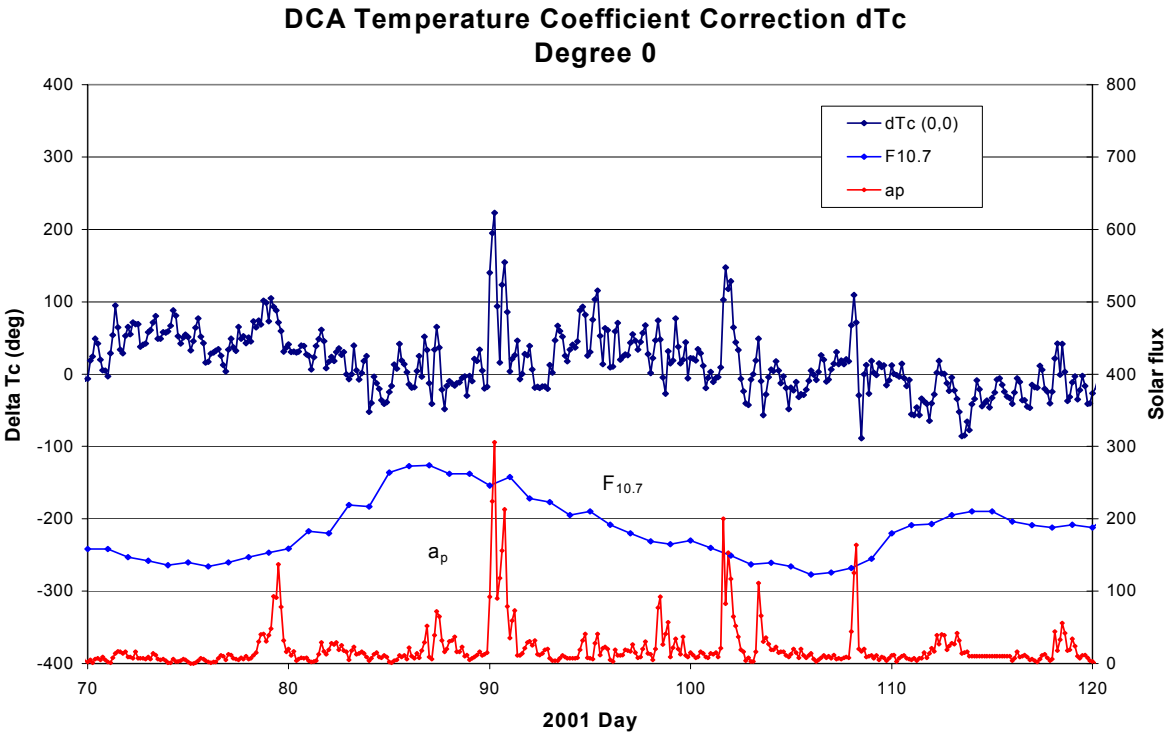

Figure 9. 2001 days 70 to 120 ΔT_c values from the degree 0 DCA 2x1 temperature field.

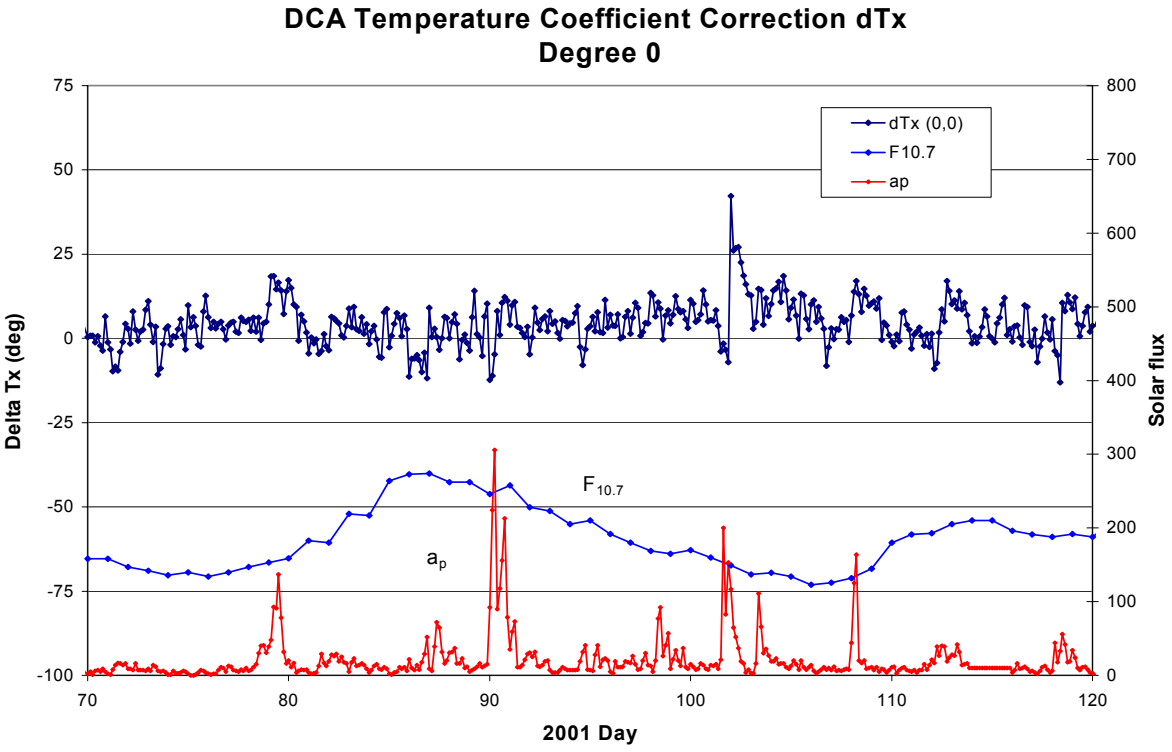

Figure 10. 2001 days 70 to 120 ΔT_x values from the degree 0 DCA 2x1 temperature field.

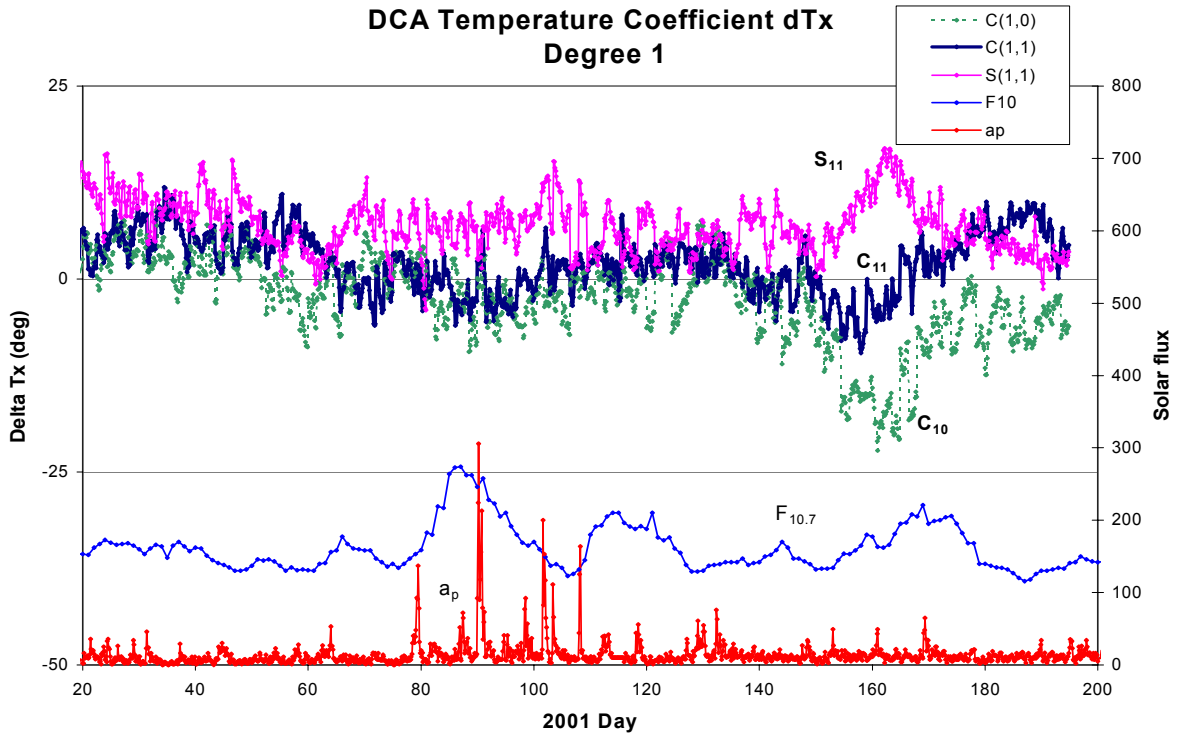

Figure 11. 2001 days 20 to 200 ΔT_x values from the degree 1 DCA 2x1 temperature field.

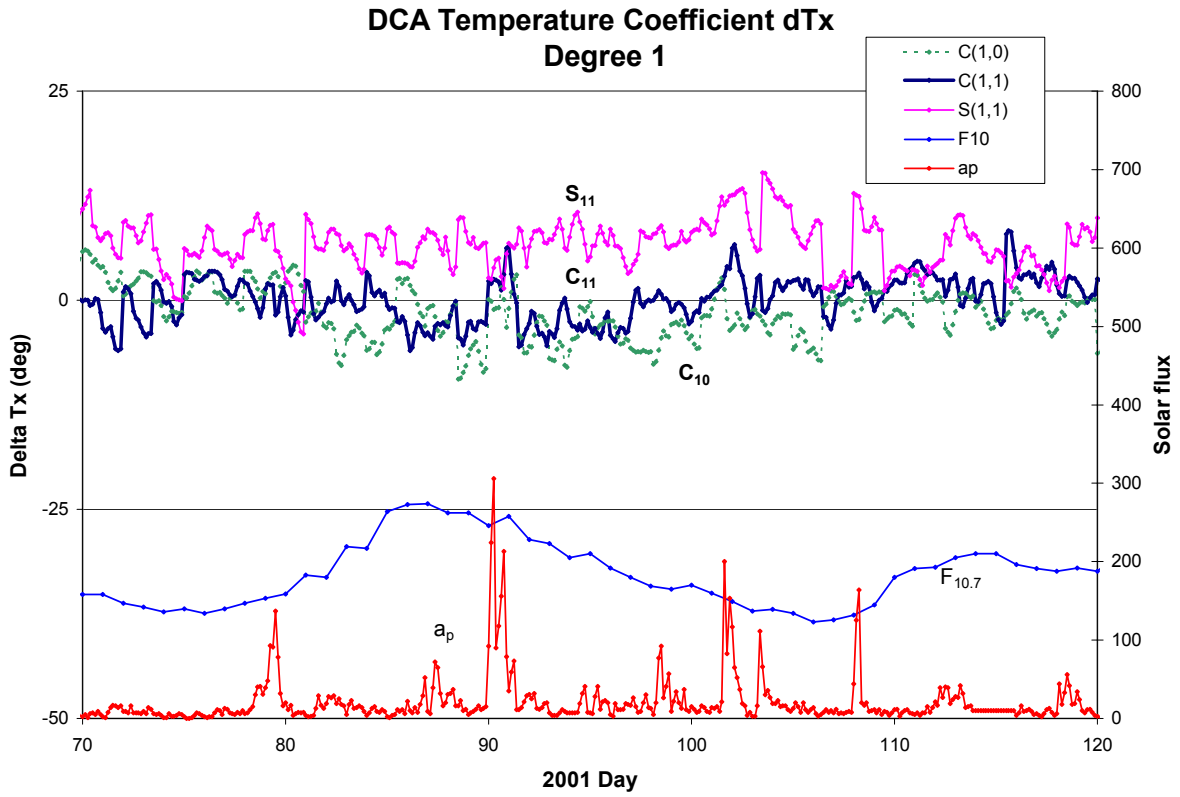

Figure 12. 2001 days 70 to 120 ΔT_x values from the degree 1 DCA 2x1 temperature field.